Nucleon-nucleon elastic scattering at large transverse momentum

J. Szwed
Max-Planck-Institut für Physik und Astrophysik, München, Federal Republic of Germany and Institute of Computer Science, Jagellonian University, Kraków, Poland
(Received 15 October 1980; revised manuscript received 11 February 1981)

Elastic scattering of nucleons is studied by classifying quark-gluon diagrams of quantum chromodynamics. Three classes of diagrams are explicitly constructed. They differ among each other depending on the way in which the momentum is transferred from one nucleon to the other. Energy, angle, flavor, and crossing dependence of these amplitudes have been calculated and compared with all large-momentum-transfer data. In the large-angle region the quark-interchange diagrams dominate and give an excellent description of experiments when the interchanged quarks interact. The Fermilab and CERN ISR region is well described by the gluon-exchange diagram. Spin effects are calculated with two alternative structures of interaction within the nucleon. Recent measurements suggest s-channel helicity conservation in the whole elastic amplitude.

I. INTRODUCTION

Exclusive processes offer an appealing possibility of a complex investigation of strong interactions. One has the possibility to observe the scattering of particle constituents; in addition the process depends crucially on the hadronic wave function. This fact makes the analysis more complicated; on the other hand there are many observable and very well measured[1-4] quantities which one obtains once the scheme is set up. These processes form therefore another set of tests of theory in addition to the standard ones in inclusive scattering.

In the paper we study elastic scattering of nucleons at large transverse momentum. We divide the quantum-chromodynamics (QCD) diagrams of this process into groups which are distinguished by the way the momentum flows from one nucleon to the other. We focus our attention on the interaction of quarks coming from different nucleons.

The interaction of constituents within a single hadron is assumed to be summed up in the nucleon form factor. First we analyze observables which are very weakly spin dependent. These are the differential cross sections $d\sigma/dt$ as a function of the c.m. energy $\sqrt{s}$ and momentum transfer t. We assume that we are allowed to use the hard-scattering techniques for $|t| \geq 5$ GeV^2. Above this value the nucleon form factor shows $1/t^2$ behavior[5] (Fig. 1), a form which was predicted by the dimensional-counting rules[6] for the region where masses are negligible. The main conclusion of this part is that the large-angle ($s \approx -t$) region is very well described by the diagrams with interchanged and interacting quarks. In the Fermilab and CERN ISR region ($|t| \ll s$) there is a clear need for gluon-exchange diagrams. The simple version of the quark-interchange mechanism gives to weak angular dependence in the region where it is dominating.

The spin of all constituents plays a crucial role in the process. Even the exact form of the quark-quark amplitude does not determine the spin dependent quantities. We consider here two possibilities concerning the spins of the uninterchanged quarks. They correspond to different types of interactions within a single nucleon (soft or hard). They are clearly distinguished by the spin-spin asymmetries at large angles. Present data on these quantities[3] suggest the s-channel helicity conservation in the whole process.

In this scheme there appear only two free constants—the normalizations of two contributions to the amplitude. They are essentially given by the number of diagrams contributing to each group.

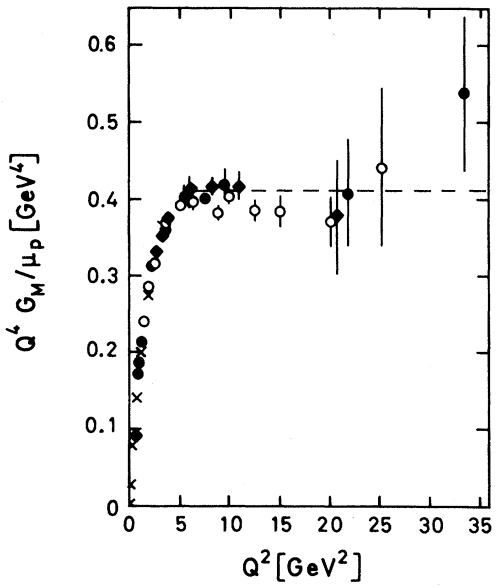

FIG. 1. The proton form factor $G_M(Q^2)$. The broken line represents the $1/Q^4$ behavior.

The paper is organized as follows. In Sec. II the assumptions of the scheme are given and the quark-quark amplitude is discussed. The spin formalism is introduced in Sec. III. The comparison with the data and discussion of the resulting consequences is given in Sec. IV. Conclusions and open problems close the paper.

II. TYPES OF DIAGRAMS AND QUARK-QUARK SCATTERING

The exact calculation of the nucleon-nucleon scattering seems to be difficult even if a calculation technique is given (e.g., Ref. 7). This is partly due to the very large number of diagrams contributing to the process. In the following we shall distinguish three groups of graphs which will be studied. The criterion is the way in which the momentum flows from one hadron to the other. It can be transferred via the quark lines, gluon lines, or quark and gluon lines simultaneously. The first group of diagrams [Fig. 2(a)] forms the basis of the quark-interchange model[8] (QIC). The hadrons interchange two quark lines which are not directly connected. The whole diagram is, of course, connected but we do not display the interaction within the hadrons. The gluon exchanges there, soft and hard ones, give rise to the wave function and effectively build up the nucleon form factor. The QIC nucleon amplitude can thus be written in the form

$$\mathfrak{M}(s,t)=M(s,t)F(t)F(u)+(t\leftrightarrow u)\,. \tag{1}$$

$M(s,t)$ is the quark-quark scattering amplitude and F is the nucleon form factor. The spin indices are suppressed in $\mathfrak{M}$; they will be discussed in detail in the next section. Because the interchanged quarks do not interact, the only nonzero quark helicity amplitudes are

$$M_{++++}(s,t)=-M_{-++-}(s,t)=1\,. \tag{2}$$

The graphs of the type (1) are expected to dominate in the region where $s\sim -t$.

There exists another set of diagrams which should be important in the same region. The momentum is transferred there by the interchange of quarks, which additionally exchange a gluon line [Fig. 2(b)]. This line cannot be absorbed into the wave function and has to be treated explicitly. This contribution, which we call QIA, has the form of (1) with the quark amplitudes

$$M_{++++}(s,t)=\tfrac{16}{3}\pi\alpha_s\frac{s}{u}\,,$$
$$M_{-++-}(s,t)=\tfrac{16}{3}\pi\alpha_s\frac{t}{u}\,. \tag{3}$$

The use of the Born term is justified only for s, and t large and $s\sim -t$. It turns out that the above conditions are satisfied in the region where this contribution dominates.

Both QIC and QIA terms are present in the QCD scheme of Brodsky and Lepage.[7] In that approach one writes the nucleon-nucleon amplitude as a convolution of the wave functions $\phi(x,p_\perp)$ and the hard-scattering amplitude $T_H(x,p_\perp{}^2)$

$$\mathfrak{M}_{AB\to CD}=\int\{dx_i\}\phi_C^\dagger(x_C,p_\perp)\phi_D^\dagger(x_D,p_\perp)\times T_H(x_i,p_\perp{}^2)\phi_A(x_A,p_\perp)\phi_B(x_B,p_\perp)\,. \tag{4}$$

In the leading form T_H is the three-quark–three-quark scattering amplitude and contains the minimal number of gluon exchanges which make the diagram connected (Fig. 3). One can regard the gluon lines as the contribution to the form factors (QIC type) unless one of the lines connects two interchanged quarks (QIA type). The form (1) follows from (4) when the $p_\perp$ inside the nucleons are limited.

The third group contributing to nucleon-nucleon scattering is composed of the diagrams with pure gluonic exchange in the t channels (GEX). We consider here only those in which the momentum transfer goes from a single quark in one hadron to a single quark in the other hadron [Fig. 2(c)]. This enables us to write the nucleon amplitude

$$\mathfrak{M}(s,t)=M(s,t)F^2(t)+(t\leftrightarrow u)\,. \tag{5}$$

In the quark amplitude $M(s,t)$ one has to exchange at least two gluon lines in order to keep the final hadrons colorless. We use the form calculated by

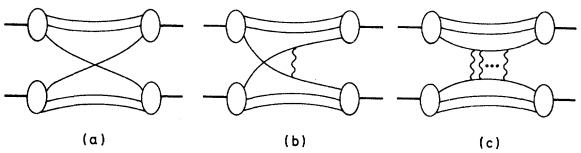

FIG. 2. Three classes of diagrams contributing to the nucleon-nucleon scattering: (a) the quark-interchange (QIC) term, (b) the quark-interchange and -interaction (QIA) term, (c) the gluon-exchange (GEX) term.

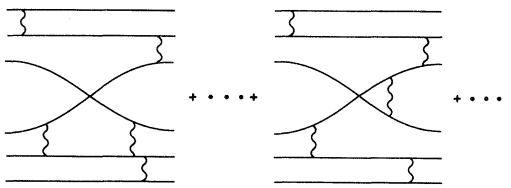

FIG. 3. Diagrams contributing to the amplitude T_H of Eq. (4).

Carruthers, Fishbane, and Zachariasen[9]:

$$M(s,t) \propto \frac{i}{\ln s} M_{\text{Born}}(s,t) . \tag{6}$$

It is the color-singlet solution of the integral equation of the Cornwall-Tiktopoulos[10] type, constructed in agreement with the known perturbative results. It is not obvious that the above form is correct due to leading-logarithmic approximation used in the calculation. This is, however, the only known solution in the limit of large s and t. We expect the term (5) to play an important role at Fermilab and ISR energies where $s \gg |t|$.

The nucleon form factor which is needed in the amplitude was calculated in QCD by Brodsky and Lepage[7] and reads

$$F_M(Q^2) \propto \left[\frac{\alpha_s(Q^2/\Lambda^2)}{Q^2}\right]^2 \left(\ln\frac{Q^2}{\Lambda^2}\right)^{-4/3\beta} , \tag{7}$$

where $\beta = (33 - 2f)/3$ and f is the number of flavors. The QCD correction to the old dimensional-counting prediction[6]

$$F_M(Q^2) \propto \frac{1}{Q^4} \tag{8}$$

is not seen in the data (Fig. 1). In order thus to concentrate on the dynamics of the scattering we assume Λ to be small enough to make Eq. (7) compatible with (8) and the data.

All above-mentioned contributions to the cross section behave in a similar way at fixed angle

$$\frac{d\sigma}{dt} \propto \frac{1}{s^{10}} F(\theta_{\text{c.m.}})$$

up to logarithmic factors. Their behavior is, however, completely different at fixed t or s. The QIC and QIA terms fall off very fast with energy at given t ($\propto 1/s^{4-6}$), whereas the GEX term is nearly constant ($\propto 1/\ln^2 s$). At fixed energy the GEX part shows strong dependence on t ($\propto 1/t^{10}$), the two remaining very much weaker. This enables us to conjecture that the gluon-exchange and quark-interchange-interaction terms contribute to different regions of $\theta_{\text{c.m.}}$.

The above remarks form a framework of our scheme. One sees that the proposed technique does not consist in exact evaluation of diagrams of the type shown in Figs. 2 and 3. It corresponds to the limiting case when the interchanged quark carries a large fraction of proton momentum ($x \to 1$). This is also the reason why we consider only three groups of diagrams shown schematically in Fig. 2. In general there are also diagrams where, in addition to the hard-scattering part, the remaining (spectator) quarks exchange gluons between the nucleons. In our case these quarks have $x \approx 0$ and "there is no time" for this additional, soft interaction.

Another contribution to elastic scattering in which all quarks of one nucleon scatter off all quarks of the other nucleon was considered by Landshoff.[11] It gives rise to the region where $|t| \ll s$ and thus should be added to our GEX term. One notices that the Landshoff diagram is real, therefore there are no interference effects in this region.

A crucial step in the construction of the amplitude is the inclusion of quark spin and favor.

III. SPIN AND FLAVOR DEPENDENCE

Nucleon-nucleon elastic scattering is described by 16-spin amplitudes. Parity conservation and time-reversal invariance reduce the number of independent amplitudes to six. In the Jacob and Wick convention,[12] assuming the scattering in the xz plane,

$$\begin{aligned}
&\phi_1 = \mathfrak{M}_{++++} = \mathfrak{M}_{----} , \\
&\phi_2 = \mathfrak{M}_{--++} = \mathfrak{M}_{++--} , \\
&\phi_3 = \mathfrak{M}_{+-+-} = \mathfrak{M}_{-+-+} , \\
&\phi_4 = \mathfrak{M}_{-++-} = \mathfrak{M}_{+--+} , \\
&\phi_5 = \mathfrak{M}_{+++-} = -\mathfrak{M}_{---+} = -\mathfrak{M}_{+-++} = \mathfrak{M}_{-+--} , \\
&\mathfrak{M}_{++-+} = -\mathfrak{M}_{--+-} = -\mathfrak{M}_{-+++} = \mathfrak{M}_{+---} .
\end{aligned} \tag{9}$$

Identical-particle symmetry imposes one additional relation $\mathfrak{M}_{++-+} = -\mathfrak{M}_{--+-}$. Assuming SU(6) spin-flavor symmetry for the nucleon wave function, one gets for the pp amplitude in QIC and QIA,

$$\begin{aligned}
\mathfrak{M}_{++++}(s,t) &= \tfrac{1}{9}[31M_{++++}(s,t) + 14M_{+-+-}(s,t) \\
&\quad + 31M_{++++}(s,u) + 14M_{+-+-}(s,u)]F(t)F(u) , \\
\mathfrak{M}_{--++}(s,t) &= \tfrac{1}{9}[17M_{--++}(s,t) + 17M_{--++}(s,u)]F(t)F(u) , \\
\mathfrak{M}_{+-+-}(s,t) &= \tfrac{1}{9}[31M_{+-+-}(s,t) + 14M_{++++}(s,t) \\
&\quad - 17M_{-++-}(s,u)]F(t)F(u) , \\
\mathfrak{M}_{-++-}(s,t) &= \tfrac{1}{9}[17M_{-++-}(s,t) - 31M_{+-+-}(s,u) \\
&\quad - 14M_{++++}(s,u)]F(t)F(u) , \\
\mathfrak{M}_{+++-}(s,t) &= 0 .
\end{aligned} \tag{10}$$

The np elastic amplitudes are given in Appendix B. In order to get the gluon-exchange part (GEX) one has to multiply in (10) the quark amplitudes $M(s,t)$ by $F^2(t)$ and $M(s,u)$ by $F^2(u)$ instead of the common factor $F(t)\,F(u)$.

Equations (10) use the fact that the total momentum transfer occurs at the quark-quark level. They contain also very important information about the spin structure of the amplitude—the helicity dependence of the proton amplitude is given by that of the quark amplitude. This means that the re-

maining valence (spectator) quarks conserve their spin projections. The last statement is strongly frame-dependent. One has to state explicitly in which spin system the relations (10) hold. In the following we consider two cases differing by the choice of the spin frame for (10). The first one assumes the s-channel helicity conservation for all quark lines. This is obvious for the quark-quark scattering amplitude $M(s,t)$ where high-energy massless quarks interact via the exchange of vector particles (the QIA and GEX cases) or do not interact at all (QIC). The assumption requires, however, the interaction within the nucleon to fulfill the same conditions. An example of a scheme which contains the above feature is the approach of Brodsky and Lepage where the amplitude T_H in (4) contains only hard exchanges of gluons.

In this case the pp amplitudes simplify to[16]

$$\begin{aligned}
\phi_1(s,t) &= \tfrac{1}{9}[31M_{++++}(s,t)+31M_{++++}(s,u)]F(t)F(u)\,,\\
\phi_3(s,t) &= \tfrac{1}{9}[14M_{++++}(s,t)-17M_{-++-}(s,u)]F(t)F(u)\,,\\
\phi_4(s,t) &= \tfrac{1}{9}[17M_{-++-}(s,t)-14M_{++++}(s,u)]F(t)F(u)\,,\\
\phi_2(s,t) &= \phi_5(s,t) = 0\,.
\end{aligned} \tag{11}$$

One can take for the quark amplitudes $M(s,t)$ the form (2)—this is then the QIC_s contribution (the index s denotes s-channel helicity conservation) or the form (3) in order to get the QIA_s part. A similar procedure can be applied to the GEX part. The above step completes the construction of the amplitude.

The second case under consideration is based on the conjecture that the interaction within the nucleon is not necessarily hard. It is then not obvious that the spectator quarks conserve the s-channel helicity—the exact dynamics is not known. We accept here the impulse approximation: during the quark-quark collision or interchange the remaining valence quarks move freely and conserve their spin projections onto the direction of motion. One has therefore to write Eqs. (10) in a frame where the spectator quarks move without changing forward direction. Such a frame is called the Gottfried-Jackson (GJ) frame.[13] Its use is very successful in low-$p_\perp$ physics and many arguments in favor of it have been given.[14]

Let us construct, for example, the pp helicity amplitudes in the $\mathrm{QIC}_{\mathrm{GJ}}$ case. One starts with the known helicity amplitudes (2) and rotates them to the Gottfried-Jackson frame,

$$\begin{aligned}
M^{\mathrm{GJ}}_{cdab}(s,t) = \sum_{a'b'c'd'} & d^{1/2}_{aa'}(\theta^a_{\mathrm{GJ}})d^{1/2}_{bb'}(\theta^b_{\mathrm{GJ}})\\
&\times d^{1/2}_{cc'}(\theta^c_{\mathrm{GJ}})d^{1/2}_{dd'}(\theta^d_{\mathrm{GJ}})M_{a'b'c'd'}(s,t)\,.
\end{aligned} \tag{12}$$

The angles θ^i are fixed by the kinematics of scattering and the nucleon mass m_N,

$$\cos\theta_{\mathrm{GJ}} = \pm\left(\frac{st}{(s-4m_N^2)(t-4m_N^2)}\right)^{1/2}. \tag{13}$$

The upper sign holds for the initial particles, the lower for the final ones (more details concerning the Gottfried-Jackson frame are given in Appendix A).

Putting (12) into (10) one obtains the proton amplitudes in the Gottfried-Jackson frame. In order to get the helicity amplitudes $M(s,t)$ one rotates the amplitudes $M^{\mathrm{GJ}}(s,t)$ back to the helicity frame—the rotation angles θ^i change only the sign. In the case of $\mathrm{QIC}_{\mathrm{GJ}}$ the result with the use of (2) reads

$$\begin{aligned}
\phi_1(s,t) &= \tfrac{1}{9}[34+a(s,t)+a(s,u)]F(t)F(u)\,,\\
\phi_2(s,t) &= \tfrac{1}{9}[28-a(s,t)-a(s,u)]F(t)F(u)\,,\\
\phi_3(s,t) &= \tfrac{1}{9}[31+a(s,t)-a(s,u)]F(t)F(u)\,,\\
\phi_4(s,t) &= \tfrac{1}{9}[-31+a(s,t)-a(s,u)]F(t)F(u)\,,\\
\phi_5(s,t) &= 0\,,\\
a(s,t) &= 14\sin^2\theta_{\mathrm{GJ}}\,.
\end{aligned} \tag{14}$$

The $\mathrm{QIC}_{\mathrm{GJ}}$ and $\mathrm{GEX}_{\mathrm{GJ}}$ proton amplitudes obtained in the same way are given in Appendix A.

We stress at this point that in principle there is a continuum of spin frames in which one can write the relations (10), each one corresponding to another dynamics within the nucleon. We consider here only two for which one has some physical arguments.

Having explicitly constructed the amplitude we compare it with the data. We have at our disposal the differential cross section $d\sigma/dt$ as a function of energy and momentum transfer and ratios of the cross sections $\sigma(np)/\sigma(pp)$ and $\sigma(pp)/\sigma(\bar{p}p)$ at large angles. The spin structure can be analyzed by looking at the polarization

$$P = \frac{-2\,\mathrm{Im}[(\phi_1+\phi_2+\phi_3-\phi_4)\phi_5^*]}{|\phi_1|^2+|\phi_2|^2+|\phi_3|^2+|\phi_4|^2+4|\phi_5|^2} \tag{15}$$

and spin-spin asymmetries

$$A_{ii} = \frac{d\sigma(\uparrow\uparrow)+d\sigma(\downarrow\downarrow)-d\sigma(\uparrow\downarrow)-d\sigma(\downarrow\uparrow)}{d\sigma(\uparrow\uparrow)+d\sigma(\downarrow\downarrow)+d\sigma(\uparrow\downarrow)+d\sigma(\downarrow\uparrow)}\,, \tag{16}$$

where $i=(n,t,s)$ is the direction of the spin projection in the direction perpendicular to the scattering plane (n) (y axis), in the direction of motion (t) (x axis), and sideways (s) (z axis). We expect the spin observables to distinguish between the hypotheses concerning the spectator quarks.

IV. PHENOMENOLOGICAL ANALYSIS

A. Differential cross sections

The three classes of nucleon-nucleon diagrams considered should be added up in order to obtain

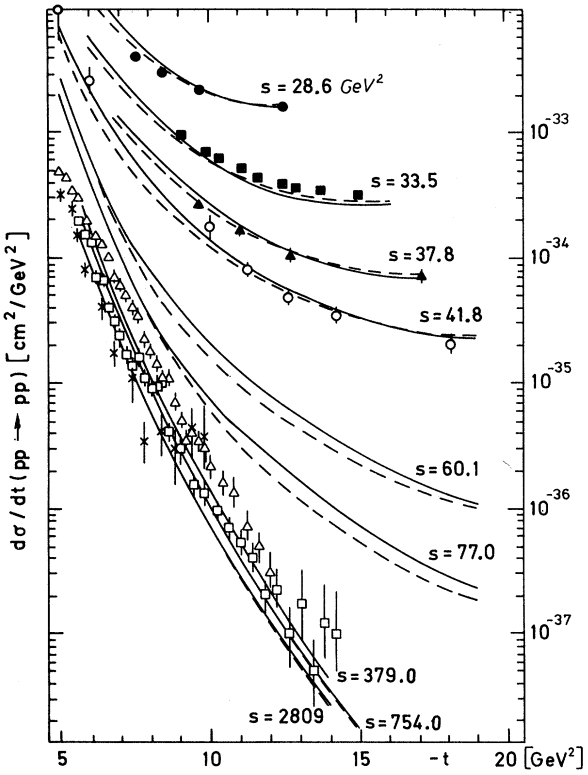

FIG. 4. The differential cross section $d\sigma/dt$ as a function of t at different energies. The solid line corresponds to the $(\mathrm{QIA}+\mathrm{GEX})_{\mathrm{GJ}}$ amplitudes, the dashed line to the $(\mathrm{QIA}+\mathrm{GEX})_s$ amplitudes.

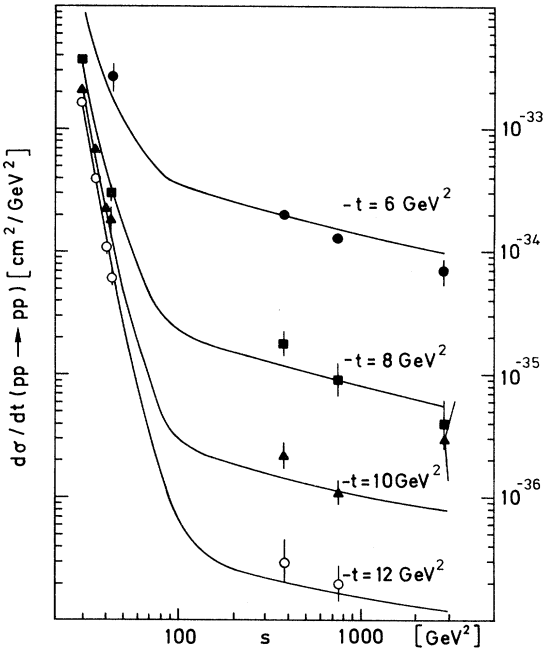

FIG. 5. The differential cross section $d\sigma/dt$ for $pp \to pp$ as a function of s at different t. The lines correspond to QIA + GEX amplitudes.

the full cross section. We expect, however, the QIC and QIA contribution to dominate in the same region of s and t and therefore investigate them separately. We begin the analysis with the QIA and GEX terms. The normalizations of both terms are left free; they depend strongly on the number of diagrams in each group. They are the only two free parameters:

$$\frac{d\sigma}{dt} = A\left[\sum_{i=1}^{4} |\phi_i^{\mathrm{QIA}}(s,t)|^2 + 4|\phi_5^{\mathrm{QIA}}(s,t)|^2\right] + B\left[\sum_{i=1}^{4} |\phi_i^{\mathrm{GEX}}(s,t)|^2 + 4|\phi_5^{\mathrm{GEX}}(s,t)|^2\right], \quad (17)$$

ϕ_i $(i=1,\ldots,5)$ of both types is given by (3), (6), and (A3). The resulting curves are shown in Figs. 4 and 5 for the laboratory momentum[1,2] $p_\perp$ = 14.3, 16.9, 19.2, 21.3, 30, 40, 201, 400, and 1496 GeV/c and $|t| > 5$ GeV^2. Both energy and angular dependence are in excellent agreement with experiment. The QIA and GEX terms contribute to separate regions of s and t. The first one governs the large-angle ($\theta_{\mathrm{c.m.}} > 50°$) scattering,[1] the second one dominates the Fermilab and ISR region[2] ($s \gg |t|$). In the last case the very slow decrease of the cross section with energy at fixed t comes entirely from the $1/\ln s$ term in the amplitude (6). The shown amplitudes interfere only at 21.3, 30, and 40 GeV/c for $|t| < 10$ GeV^2. This interference improves clearly the $s = 41.8$ GeV^2 line. The cross section (17) shows nearly no dependence on the assumption concerning the spectator quarks. The s channel and Gottfried-Jackson helicity versions of (17) do not differ as seen in Fig. 4. The ratio of the normalization parameters A and B is given in Table I. The QIC term has similar structure to the QIA part and dominates therefore in the same region of angles. We show the cross section (17) with the part QIA replaced by QIC in Fig. 6. Its agreement with the data is worse, in particular the angular dependence. We realize, however, that both QIA and QIC terms should be added up and only their sum builds up the full amplitude in this region. As in the previous case the cross section is insensitive to what happens to the spectators.

TABLE I. The ratio of the normalization constants A and B of QIA, QIC, and GEX terms in the cross-section formula (17).

	A/B	
	QIA+GEX	QIC+GEX
s	4.52×10^3	1.72×10^4
GJ	2.76×10^4	6.24×10^4

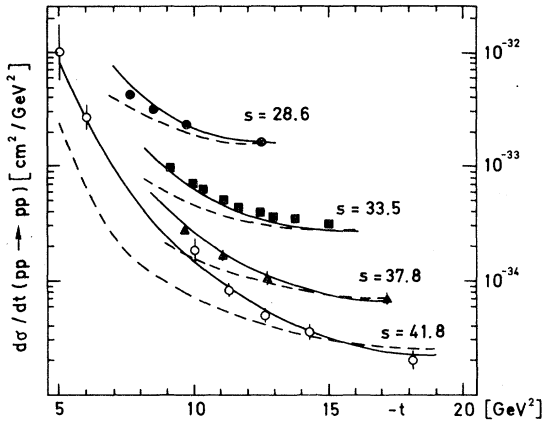

FIG. 6. The differential cross section $d\sigma/dt$ for $pp \to pp$ as a function of t at different energies. The solid line represents the QIA + GEX contribution, the dashed line represents the QIC + GEX contribution.

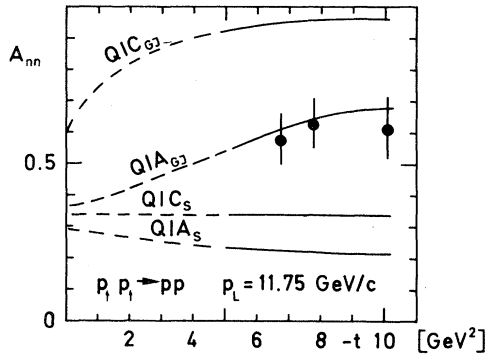

FIG. 7. The spin-spin asymmetry A_{nn} for $pp \to pp$ at 11.75 GeV/c as a function of t. The data are taken from Crabb *et al.* (Ref. 3).

B. Spin-spin asymmetries

The measured value of A_{nn} at 11.75 GeV/c (Ref. 3) offers an intriguing possibility of discriminating between the possible spin frames for Eqs. (10). One can express A_{nn} in terms of helicity amplitudes ϕ_i,

$$A_{nn} = 2\,\mathrm{Re}(\phi_1\phi_2^* - \phi_3\phi_4^* + 2|\phi_5|^2)/D$$

and similarly

$$A_{ss} = 2\,\mathrm{Re}(\phi_1\phi_2^* + \phi_3\phi_4^*)/D\,,$$

$$A_{ll} = (-|\phi_1|^2 - |\phi_2|^2 + |\phi_3|^2 + |\phi_4|^2)/D\,,$$

$$A_{sl} = 2\,\mathrm{Re}[(\phi_1 + \phi_2 - \phi_3 + \phi_4)\phi_5^*]/D\,,$$

$$D = |\phi_1|^2 + |\phi_2|^2 + |\phi_3|^2 + |\phi_4|^2 + 4|\phi_5|^2\,.$$

We show the resulting pp curves at 11.75 GeV/c (Figs. 7 and 8).[15] According to the previous subsection, the GEX term plays no role at this energy, the two remaining terms are considered separately. One notices that all spin asymmetries are given then uniquely, without free parameters. The s-channel helicity curves were obtained previously in Ref. 16. One sees clearly that the very large spin-spin asymmetry A_{nn} can be accounted in a hard-scattering process by the assumption about the Gottfried-Jackson helicity conservation for the spectators. However, even in this case the rapid change of A_{nn} with $p_\perp$ is not reproduced. We com-

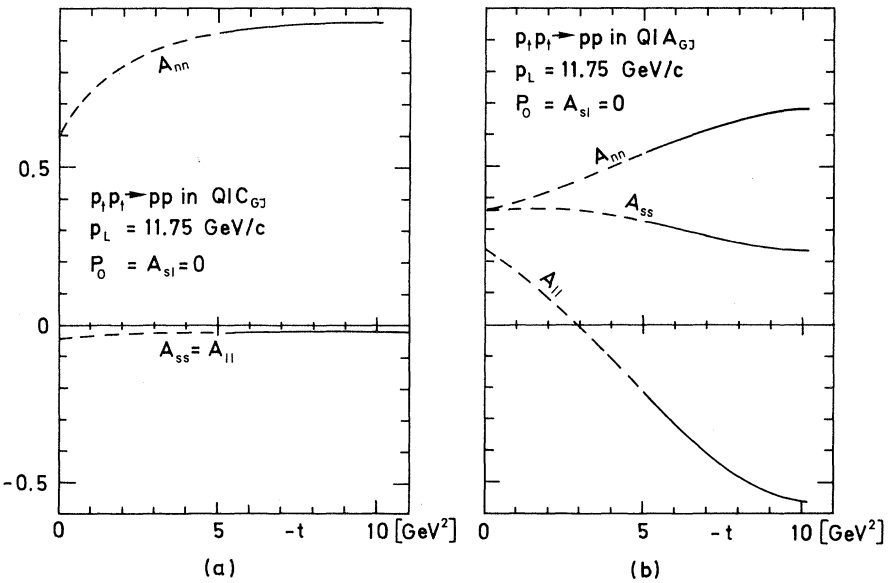

FIG. 8. Spin-spin asymmetries for $pp \to pp$ at 11.75 GeV/c as a function of t. The curves represent (a) the QIC_{GJ} term, (b) the QIA_{GJ} term.

ment on this in Sec. III C.

The astonishingly large value of A_{nn} is worth comment. The effect is explicitly seen when using the transversity amplitudes N_{abcd}.[17] In this representation both the spectator and interacting quarks conserve their transversities (the spin projections in the direction perpendicular to the scattering plane). If the nucleons have parallel transversities only quarks with parallel transversities can interact (only $N_{++++}=0$); otherwise a state $s=\frac{3}{2}$ is produced. If, however, the nucleons have opposite transversities both N_{++++} and N_{-++-} contribute. Their interference in the nucleon amplitude depend on the frame in which the quark amplitudes are related to the nucleon ones or, in other words, in which the spectator quarks conserve their transversities. In particular, these amplitudes nearly cancel in the Gottfried-Jackson frame. This causes the scattering of protons with antiparallel transversities much weaker than that with parallel transversities.

The smallness of A_{nn} in the QIC_s or QIA_s approach is partly due to the value of ϕ_2 which vanishes there. This fact can be relatively easily measured; $\phi_2=\phi_5=0$ implies

$$A_{nn}=-A_{ss}\,. \tag{18}$$

On the other hand $\phi_2\neq 0$ in the GJ approach and relation (18) is strongly violated as seen in Figs. 8.

The values of spin-spin asymmetries in np scattering are plotted in Fig. 9. A_{nn} is negative at smaller t in agreement with the measurements at 6 GeV/c.[18] We do not, however, consider this as conclusive because the momentum transfer is too low to trust the hard-scattering picture. The opposite sign of A_{nn} as comparing to pp scattering is entirely due to the difference in the flavor part of proton and neutron wave function.

We remark that the above results on spin-spin asymmetries do not change qualitatively with energy, in particular A_{nn} remains very large at 90°. One notices that both QIA and QIC terms separately give wrong values of A_{ll} when compared to preliminary data at $p_L=11.75$ GeV/c.[3]

C. Interference effects

The large angle region where $|t|/s\sim 1$ is dominated by two types of amplitudes, QIC and QIA. Their relative magnitude is given essentially by the number of diagrams contributing to both groups. In the above analysis we investigated the two contributions separately in order to see exactly their structure. The total amplitude in this region of s and t is, however, a coherent sum of both terms. This fact influences strongest the spin-spin asymmetries. One notices easily where the dependence comes from. In the s-channel helicity approach, for instance, the quark-quark amplitudes look then as follows:

$$M_{++++}(s,t)=\beta M^{\mathrm{QIC}}_{++++}(s,t)+M^{\mathrm{QIA}}_{++++}(s,t)$$
$$=\beta+\tfrac{16}{3}\pi\alpha_s\frac{s}{u}\,,$$

$$M_{-++-}(s,t)=\beta M^{\mathrm{QIC}}_{-++-}(s,t)+M^{\mathrm{QIA}}_{-++-}(s,t)$$
$$=-\beta+\tfrac{16}{3}\pi\alpha_s\frac{t}{u}\,,$$

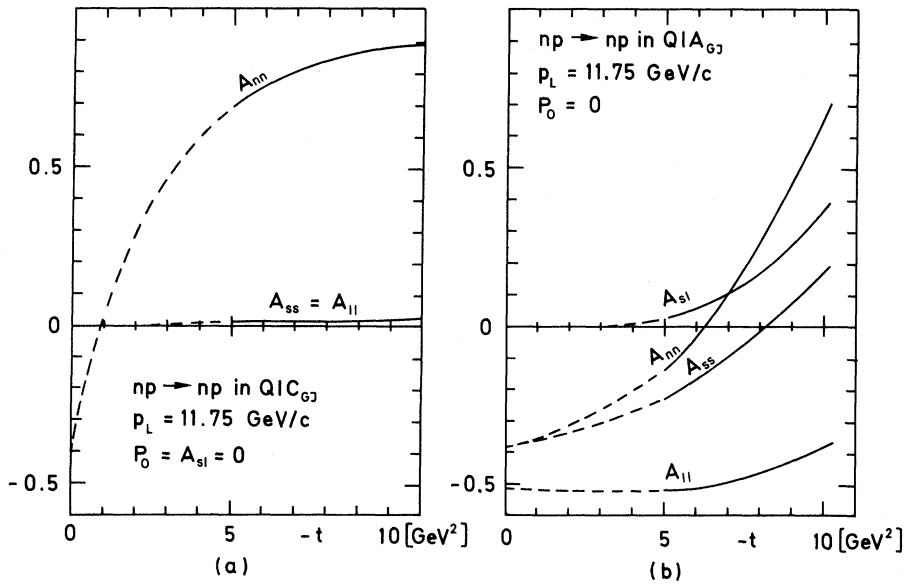

FIG. 9. The same as in Fig. 8 but for $np\to np$.

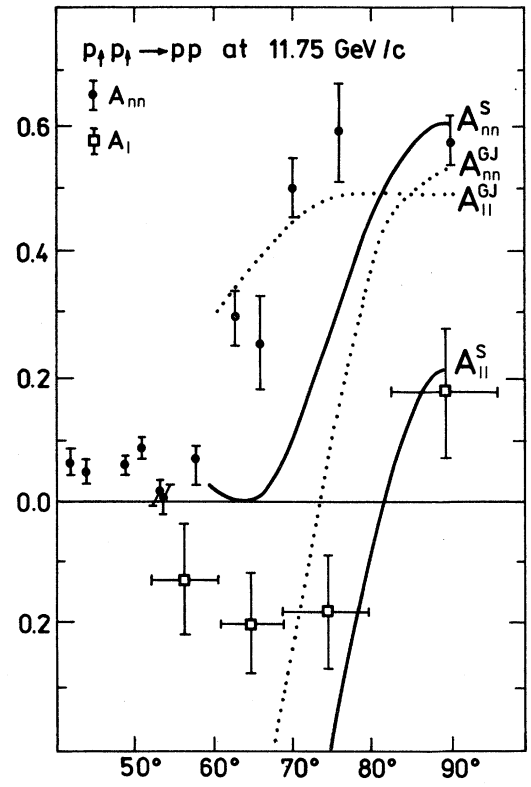

FIG. 10. Angular distribution of A_{nn} and A_{ll}. In the GJ case $=33.2\alpha_s$, in the s case $=34.9\alpha_s$.

where β gives the relative magnitude of QIC and QIA terms. The ratio M_{-++-}/M_{++++} depends now crucially on β and so do the spin-spin asymmetries. The parameter β is fixed by fitting the calculated A_{nn} and A_{ll} to the measured points at $p_L = 11.75$ GeV/c and $\theta_{c.m.} = 90°$. The resulting curves are shown in Fig. 10 for both s and GJ cases. One sees that the asymmetries clearly distinguish the two possible structures of the amplitude. However, we are aware of the fact that the energy in the process is still too low to separate unambiguously the hard-scattering region and draw final conclusions. Relatively low-momentum transfer admits an admixture of soft scattering which can play a role at lower angles (this possibility is considered in the second paper of Ref. 16). This is the reason why we expect the hard amplitude to describe only approximately the angular distribution of asymmetries at this energy.

D. Flavor and crossing dependence

Another test of the hard nucleon-nucleon amplitude is its flavor and crossing dependence. In the case of s-channel helicity conservation the problem was investigated in Refs. 16 and 19. We show the ratio $r = d\sigma/dt(np)/d\sigma/dt(pp)$ at 12 GeV/c for

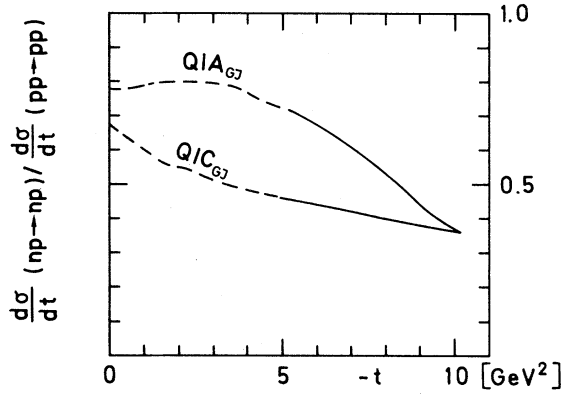

FIG. 11. The ratio of np to pp elastic differential cross sections at 11.75 GeV/c.

QIC_{GJ} and QIA_{GJ} in Fig. 11. Both forms agree very well at 90° with the measured value[4] $r = 0.34 \pm 0.04$.

Using the crossing symmetry of the amplitude one can obtain the antiproton-proton cross section at large angles by the interchange of s and u. From the measurement at 5 GeV/c (Ref. 20), one knows that the ratio $d\sigma/dt(pp)/d\sigma/dt(\bar{p}p)$ is very large. This is reproduced both in QIC and QIA as seen in Table II. An experiment at higher energy could make the picture more conclusive.

V. CONCLUSIONS

The aim of the paper was to classify possible contributions to the large-$p_\perp$ nucleon-nucleon scattering. We managed to group a large number of diagrams into three classes which differ among each other depending on the way in which the momentum is transferred from one nucleon to the other. Two of them (QIC and QIA) correspond to the summation of lowest-order diagrams of Ref. 7 in a certain limit.

It was found that the interchange of interacting quarks plus the pure gluon exchange describe the data very well. At a given energy the angular dependence of the quark-interchange diagrams is too weak; they play, however, a role in the same (s,t) region as the QIA term. One has therefore to consider the sum of both contributions.

All the considered diagrams have one common feature. The nucleon amplitude is a product of the

TABLE II. The ratio $d\sigma/dt\,(pp \to pp)/d\sigma/dt\,(\bar{p}p \to pp)$ at $\theta_{c.m.} = 90°$ and $p_L = 12$ GeV/c, obtained from the QIA and QIC terms.

	QIA	QIC
s	413.2	30.3
GJ	56.1	28.9

single quark-quark scattering amplitude and the nucleon form factors. This makes the scheme very similar to that used in low-$p_\perp$ physics.[21] There remains still a group of diagrams which avoids the above classification; all of them involve multiple quark scattering. Only some of them were investigated in detail.

We found the spin-spin asymmetries to be a very sensitive test of the spin structure of the amplitude. The assumption that the quarks within the nucleon conserve the Gottfried-Jackson helicity during the collision takes into account the fact that even in the hard-scattering region a part of the process may be soft (the hard part conserves the s-channel helicity) and leads to large A_{nn}. There are in fact theoretical arguments[22] that one is not able to factorize the hard and soft parts of the amplitude in wide-angle scattering. On the other hand, we noticed that the interference of QIA and QIC terms can produce large A_{nn}, even with the total s-channel helicity conservation. The new measurement of A_{11} at 11.75 GeV/c supports the last possibility. It is also interesting to see whether the spin effects manifest themselves in the coming experiments at higher energies or in another place (e.g., in the form factors). One notices that the analysis of other exclusive processes within this scheme is straightforward.

ACKNOWLEDGMENTS

The author would like to thank A. Białas, W. Furmański, A. Kotański, and W. Słomiński for discussions and J. Kühn for critical reading of the manuscript.

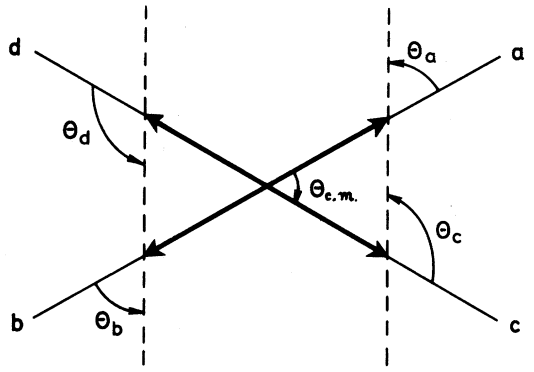

FIG. 12. The Gottfried-Jackson angles θ_i at the velocity diagram of nucleon-nucleon scattering. The solid lines represent the velocities in the s-channel c.m. system, the dashed lines the directions of velocities in the Gottfried-Jackson frame.

APPENDIX A: THE GOTTFRIED-JACKSON HELICITY FRAME

The frame is defined for the process $a+b\to c+d$ in the following way.

The spin of particle c (d) is projected in its rest frame onto the direction of motion of particle a (b). The spin of particle a (b) is projected onto the direction opposite to particle c (d). The angles θ_i of rotation from the s-channel helicity frame to the Gottfried-Jackson frame [Eq. (12)] are shown in the velocity diagram in Fig. 12. Their form in the general-mass case reads (e.g., for particle a)

$$\cos\theta^a=\frac{(s-m_a^2-m_b^2)(t-m_a^2-m_c^2)+2m_a^2(m_b^2+m_c^2-m_d^2-m_a^2)}{\{[s-(m_a+m_b)^2][s-(m_a-m_b)^2][t-(m_c+m_a)^2][t-(m_c-m_a)^2]\}^{1/2}} \tag{A1}$$

and reduces to the form (13) for nucleon-nucleon scattering. In this case for $t\to 0$ (forward scattering), $\theta_{GJ}\to\pi/2$ and at large energies it approaches very fast its large t-limit $\theta_{GJ}\to 0$ or π. The Gottfried-Jackson angles are equal up to $\pm\pi$ to the $s\leftrightarrow t$ crossing angles.[23]

To obtain the s-channel helicity amplitude one applies at first step the rotation by θ_i to the known quark helicity amplitudes $M(s,t)$, relates them to the nucleon amplitudes by equations of the type (10), and rotates by $-\theta_i$ the nucleon amplitudes back to the helicity frame. Only in the case of the spectator quarks being in spin-zero state does the dependence on θ drop out. The resulting unsymmetrized proton amplitudes in QIA_{GJ} case take the form

$$\begin{aligned}
\mathfrak{M}_{++++}(s,t)&=\tfrac{1}{9}\{[17+b(s,t)]M_{++++}(s,t)\\
&\quad+c(s,t)M_{-++-}(s,t)\}F(t)F(u)\,,\\
\mathfrak{M}_{--++}(s,t)&=\tfrac{1}{9}\{[-c(s,t)M_{++++}(s,t)\\
&\quad+[-14+d(s,t)]M_{-++-}(s,t)\}F(t)F(u)\,,\\
\mathfrak{M}_{+-+-}(s,t)&=\tfrac{1}{9}[b(s,t)M_{++++}(s,t)\\
&\quad+c(s,t)M_{-++-}(s,t)]F(t)F(u)\,,\\
\mathfrak{M}_{-++-}(s,t)&=\tfrac{1}{9}\{c(s,t)M_{++++}(s,t)\\
&\quad+[31-d(s,t)]M_{-++-}(s,t)\}F(t)F(u)\,,
\end{aligned} \tag{A2}$$

$$b(s,t)=14-24\cos^2\theta_{GJ}+10\cos^4\theta_{GJ}\,,$$

$$c(s,t)=-10\cos^2\theta_{GJ}\sin^2\theta_{GJ}\,,$$

$$d(s,t)=14-4\cos^2\theta_{GJ}-10\cos^4\theta_{GJ}\,,$$

where the quark amplitudes are given by (3). The t-u symmetrization implies

$$\begin{aligned}
\phi_1(s,t) &= \mathfrak{M}_{++++}(s,t) + \mathfrak{M}_{++++}(s,u)\,, \\
\phi_2(s,t) &= \mathfrak{M}_{--++}(s,t) + \mathfrak{M}_{--++}(s,u)\,, \\
\phi_3(s,t) &= \mathfrak{M}_{+-+-}(s,t) - \mathfrak{M}_{-+-+}(s,u)\,, \\
\phi_4(s,t) &= \mathfrak{M}_{-++-}(s,t) - \mathfrak{M}_{+--+}(s,u)\,, \\
\phi_5(s,t) &= 0\,.
\end{aligned} \tag{A3}$$

The $\mathrm{GEX}_{\mathrm{GJ}}$ amplitudes are obtained by using (6) for the quark amplitudes $M(s,t)$ and replacing in (A2) $F(t)F(u)$ by $F^2(t)$.

APPENDIX B: THE NEUTRON-PROTON ELASTIC AMPLITUDES

Assuming the quark interchange and s-channel helicity conservation, one obtains

$$\begin{aligned}
\phi_1(s,t) &= \tfrac{1}{18}[\,14M_{++++}(s,t) + 22M_{+--+}(s,t) \\
&\quad + 17M_{++++}(s,u) - 8M_{+--+}(s,u)\,]F(t)F(u), \\
\phi_2(s,t) &= \tfrac{1}{18}[-8M_{--++}(s,t) + 25M_{--++}(s,u)\,]F(t)F(u)\,, \\
\phi_3(s,t) &= \tfrac{1}{18}[\,22M_{+-+-}(s,t) + 14M_{+--+}(s,t) \\
&\quad - 25M_{-+-+}(s,u)\,]F(t)F(u)\,, \\
\phi_4(s,t) &= \tfrac{1}{18}[\,-8M_{-++-}(s,t) - 17M_{+--+}(s,u) \\
&\quad + 8M_{++++}(s,u)\,]F(t)F(u)\,, \\
\phi_5(s,t) &= \tfrac{1}{18}[-8M_{++--}(s,t) - 25M_{+--+}(s,u)\,]F(t)F(u)\,.
\end{aligned} \tag{B1}$$

In case of QIC_s or QIA_s one replaces the quark amplitudes by (2) or (3). In both cases only M_{++++} and M_{-++-} survive. GEX_s amplitudes are obtained by replacing in (B1) the form factors by $F^2(t)$ or $F^2(u)$ and using the quark amplitudes (6) (only M_{++++} and M_{+--+} are nonzero).

The $\mathrm{QIC}_{\mathrm{GJ}}$ and $\mathrm{QIA}_{\mathrm{GJ}}$ amplitudes read

$$\begin{aligned}
\phi_1(s,t) &= \tfrac{1}{18}\{[-8+f(s,t)]M_{++++}(s,t) + 4f'(s,t)M_{-++-}(s,t) + [25+f'(s,u)]M_{++++}(s,u) + f'(s,u)M_{-++-}(s,u)\}F(t)F(u)\,, \\
\phi_2(s,t) &= \tfrac{1}{18}\{-4f'(s,t)M_{++++}(s,t) + [14+h(s,t)]M_{--++}(s,t) - f'(s,u)M_{++++}(s,u) + [8-h'(s,u)]M_{--++}(s,u)\}F(t)F(u)\,, \\
\phi_3(s,t) &= \tfrac{1}{18}\{f(s,t)M_{+-+-}(s,t) + 4f'(s,t)M_{--++}(s,t) - f'(s,u)M_{++++}(s,u) + [17+h'(s,u)]M_{--++}(s,u)\}F(t)F(u)\,, \\
\phi_4(s,t) &= \tfrac{1}{18}\{4f'(s,t)M_{++++}(s,t) + [14+h(s,t)]M_{-++-}(s,t) - f'(s,u)M_{++++}(s,u) - f'(s,u)M_{--++}(s,u)\}F(t)F(u)\,, \\
\phi_5(s,t) &= \tfrac{1}{18}\{k(s,t)M_{++++}(s,t) + l(s,t)M_{--++}(s,t) - k'(s,u)M_{++++}(s,u) - l'(s,u)M_{--++}(s,u)\}F(t)F(u)\,,
\end{aligned} \tag{B2}$$

$$f = 2\sin^2\theta_{\mathrm{GJ}}(7+4\sin^2\theta_{\mathrm{GJ}})\,, \quad k = -\sin\theta_{\mathrm{GJ}}\cos\theta_{\mathrm{GJ}}(15+8\cos^2\theta_{\mathrm{GJ}})\,,$$

$$f' = -2\cos^2\theta_{\mathrm{GJ}}\sin^2\theta_{\mathrm{GJ}}\,, \quad k' = -\sin\theta_{\mathrm{GJ}}\cos\theta_{\mathrm{GJ}}(3+2\cos^2\theta_{\mathrm{GJ}})\,,$$

$$h = -2\sin^2\theta_{\mathrm{GJ}}(15-4\sin^2\theta_{\mathrm{GJ}})\,, \quad l = -\sin\theta_{\mathrm{GJ}}\cos\theta_{\mathrm{GJ}}(7+8\cos^2\theta_{\mathrm{GJ}})\,,$$

$$h' = 2\sin^2\theta_{\mathrm{GJ}}(7+\sin^2\theta_{\mathrm{GJ}})\,, \quad l' = \sin\theta_{\mathrm{GJ}}\cos\theta_{\mathrm{GJ}}(5+2\cos^2\theta_{\mathrm{GJ}})\,.$$

The construction of $\mathrm{GEX}_{\mathrm{GJ}}$ from (B2) is straightforward.

[1] M. V. Allaby *et al.*, Phys. Lett. 25B, 156 (1967); G. Cocconi *et al.*, Phys. Rev. 138, 165 (1965).
[2] J. L. Martman *et al.* Phys. Rev. Lett. 38, 975 (1977); S. Conetti *et al.*, *ibid.* 41, 924 (1978); M. Dekerret *et al.*, Phys. Lett. 68B, 374 (1977).
[3] J. R. O'Fallon *et al.*, Phys. Rev. Lett. 39, 733 (1977); D. G. Crabb *et al.*, *ibid.* 41, 1257 (1978); I. P. Auer *et al.* Report No. ANL-HEP-CP-80-38 (unpublished).
[4] J. L. Stone *et al.* Phys. Rev. Lett. 38, 1315 (1977).
[5] M. D. Mestayer, SLAC Report No. 214, 1978 (unpublished) and references therein.
[6] S. J. Brodsky and G. R. Farrar, Phys. Rev. Lett. 31, 1153 (1973); V. A. Matveev, R. M. Muradyan, and A. V. Tavkhelidze:, Lett. Nuovo Cimento 7, 719 (1973).
[7] G. P. Lepage and S. J. Brodsky, Phys. Rev. Lett. 43, 545 (1979); Phys. Rev. D 22, 2157 (1980).
[8] R. Blankenbecler, S. J. Brodsky, and J. F. Gunion, Phys. Lett. 39B, 649 (1972); 42B, 461 (1973); Phys. Rev. D 6, 2654 (1972); 8, 287 (1973); P. V. Landshoff and J. C. Polkinghorne, *ibid.* 8, 927 (1973) 8, 4157 (1973).
[9] P. Carruthers, P. Fishbane, and F. Zachariasen, Phys. Rev. D 15, 3675 (1977).
[10] J. M. Cornwall and G. Tiktopoulos, Phys. Rev. Letters 35, 338 (1975); Phys. Rev. D 13, 3370 (1976).
[11] P. V. Landshoff, Phys. Rev. D 10, 1024 (1974).
[12] M. Jacob and G. C. Wick, Ann. Phys. (N. Y.) 7, 404 (1959).
[13] K. Gottfried and J. D. Jackson, Nuovo Cimento 33, 309 (1964).
[14] A. Białas, A. Kotański, and K. Zalewski, Nucl. Phys. B82, 1 (1971).
[15] J. Szwed, Phys. Lett. 93B, 485 (1980).
[16] G. Farrar, S. Gottlieb, D. Sivers, and G. M. Thomas, Phys. Rev. D 20, 202 (1979); S. J. Brodsky, C. E. Carlson, and M. Lipkin, *ibid.* 20, 2278 (1979).
[17] A. Kotański, Acta Phys. Pol. 29, 699 (1966); 30, 629 (1966).
[18] D. G. Crabb *et al.*, Phys. Rev. Lett. 43, 983 (1979).
[19] J. F. Gunion, S. J. Brodsky, and R. Blankenbecler, Phys. Rev. D 8, 287 (1973).

[20]V. Chabaud, Phys. Lett. 38B, 449 (1972).
[21]A. Biatas (private communication).
[22]A. Duncan and A. Mueller, Phys. Rev. D 21, 1636 (1980); A. Duncan, Columbia University Report No. CU-TP-187 (unpublished).
[23]T. L. Trueman and G. C. Wick, Ann. Phys. (N.Y.) 26, 322 (1964); G. Cohen-Tannoudji, A. Morel, and M. Navelet, *ibid.* 46, 239 (1968).
[24]I. P. Auer *et al.*, Report No. ANL-HEP-CP-80-38 (unpublished).